A SIMPLE EXPERIMENTAL DEMONSTRATION OF AEROELASTIC INSTABILITIES

Luciano Amaury dos Santos
Instituto de Aeronáutica e Espaço - CTA, Praça Mar. Eduardo Gomes, 50 – São José dos Campos – SP, Brasil, 12.228-904
e-mail: lucianosantos@iae.cta.br

Roberto Gil Annes da Silva
Instituto de Aeronáutica e Espaço – CTA, Praça Mar. Eduardo Gomes, 50 – São José dos Campos – SP, Brasil, 12.228-904
e-mail: rasilva@iae.cta.br

Breno Moura Castro
Instituto de Aeronáutica e Espaço – CTA, Praça Mar. Eduardo Gomes, 50 – São José dos Campos – SP, Brasil, 12.228-904
e-mail: breno@iae.cta.br

Adolfo Gomes Marto
Instituto de Aeronáutica e Espaço – CTA, Praça Mar. Eduardo Gomes, 50 – São José dos Campos – SP, Brasil, 12.228-904
e-mail: agmarto@iae.cta.br

Antonio Carlos Ponce Alonso
Instituto de Aeronáutica e Espaço – CTA, Praça Mar. Eduardo Gomes, 50 – São José dos Campos – SP, Brasil, 12.228-904
e-mail: ponce@iae.cta.br

Abstract. *Although the flutter of banners or of venetian blind fins exposed to wind can be observed frequently, there are not so many structures having some resemblance to an aircraft wing and that are sufficiently flexible in torsion to allow the observation of aeroelastic instabilities when exposed to air streams of low velocities. But there are rulers, made of PVC, decimals of a milimeter thick, around twenty centimeters long and four centimeters wide that have the mass and flexibility properties needed for the occurrence of flutter and/or aeroelastic divergence when exposed to air streams of relatively low velocities. These rulers are also sufficiently tough to withstand the repeated high deformations to which they are subject in such a situation. The present paper discusses a simple experiment made with a ruler of this kind, comparing the observations with theoretical predictions. Besides demonstrating the most basic types of aeroelastic instability (the divergence and the classical flutter), as well as the effect of sweep over them, this experiment calls attention to the geometrical non-linearities, associated to high deformations, and to the aerodynamic nonlinearities associated with the flow separation at the non-rounded leading edge of the ruler. It is due to the non-linearities that limit cycle oscillations are observed instead of a catastrophic flutter. The non-linearities are also responsible for avoiding the collapse of the ruler when the aeroelastic divergence speed is reached by the air stream.*

Keywords*: Aeroelasticity, Unsteady Aerodynamics, Experimental Aerodynamics, Aerodynamics Teaching*

1. Introduction

Aeroelastic instabilities occur when the airflow around a structure transfers mechanical energy to it in a manner that increases unboundedly the amplitude of initially small deformations of that structure. These instabilities may be dynamic, associated to vibration and usually known as flutter, or static, characterized by large deformations in a single direction and known as aeroelastic divergence. Aeroelastic divergence is mainly associated with lifting surfaces. Flutter occurs in a more wide range of situations, involving, for example, the tail cone and the control surfaces (if their control is reversible and they are not properly balanced[1]). These phenomena are generally cause of catastrophic aircraft failure and also have been cause of concern in airplane developments since the first years of aviation, as described by Collar (1978). Even today, flutter flight tests are one of the most dangerous stages of a new aircraft development (or integration of new external stores in a already developed aircraft). Aeroelastic wind tunnel tests frequently are part of the design cycle of new aircraft configurations. However, an aeroelastically scaled complete aircraft model is so expensive that its test is impractical for didactical purposes. An interesting remark, especially considering the popularization of the flying models design caused by the SAE Aero Design competition, is that flying models are normally too rigid for suffering from aeroelastic troubles in their flight envelope; therefore, aeroelasticity is generally disregarded in their development. As aeroelastic instabilities are not commonly seen, inexpensive and simple experiments for demonstrating their occurrence are very desirable.

[1] Hydraulic controls are virtually irreversible, but gliders and powered light weight aircraft still use long cables for control, making the balancing of control surfaces, as discussed for example in Fung (1955, sec. 5.5) and Templeton (1954), an yet important subject.

Theodorsen and Garrick (1940) conducted a somewhat interesting investigation of flutter of a typical section of a wing with a control surface, using both the theory developed by Theodorsen (1935) and wind tunnel experiments. These experiments can be reproduced at a moderate cost, but are not as safe and low cost as it would be desirable for regular laboratory classes. Frazer and Duncan (1931) developed experiments more adequate for didactical purposes, but using delicate models carefully built. In the present paper, a much inexpensive kind of experiment is proposed. In the experiments to be described here, the aeroelastic instabilities do not occur in exactly the same fashion as they would in an aircraft, but the abstraction level required to relate what is observed in these experiments to what is expected in actual flight should help the students in relating what he or she observes in a banner, a sail or a venetian blind fin that eventually flutters, with situations of more interest from the engineering standpoint.

2. Experimental setup

The basic material needed for the experiment are a thin ruler of PVC, that will be the wing model, and an air stream of measurable and controllable velocity. The air stream must reach dynamic pressures of about 15 mmH_2O, but not much more than this. The ruler can be held between the forefinger and the middle finger of somebody's hand, but an assembly, using a clamp and wood pieces like the one shown in the Fig. 1, will probably constitute a better constraint (to the model movement), easier to describe in a theoretical model.

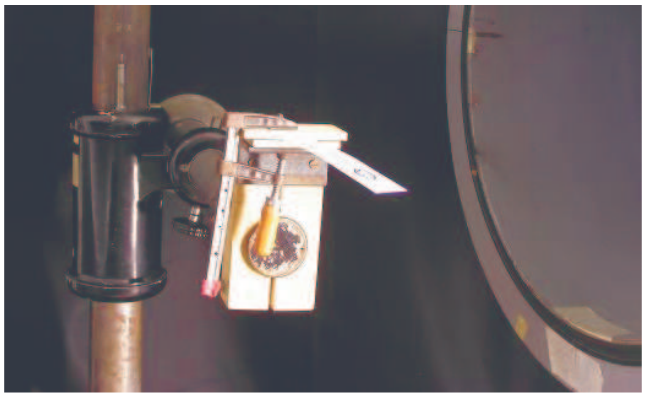

Figure 1. The experimental setup: the model is located downstream of the mouth of the wind tunnel contraction section

The experimental results, to be discussed in this paper, were obtained in the IAE/ASA-L TA-3 wind tunnel at the CTA. This tunnel has a closed circuit although it was used with its test section opened. The cylindrical mouth of its contraction section has a diameter of 65 cm. The model was positioned near the center of the jet blown by this mouth, 30 cm away from it. The dynamic pressure measured by a Pitot tube, positioned at the end of the contraction section, was used to estimate the dynamic pressure at the model position, according to the results of previous measurements using a Pitot tube place in lieu of the model.

The ruler was used to model two types of wing: one with 30 degrees of (positive) sweep angle and another with a 15 degrees negative (forward) sweep angle (prone to develop aeroelastic divergence, as explained in textbooks like that of Dowell *et al.* (1994, sec. 2.6)). The ruler positions used to represent the wings shown schematically in Fig. 2.

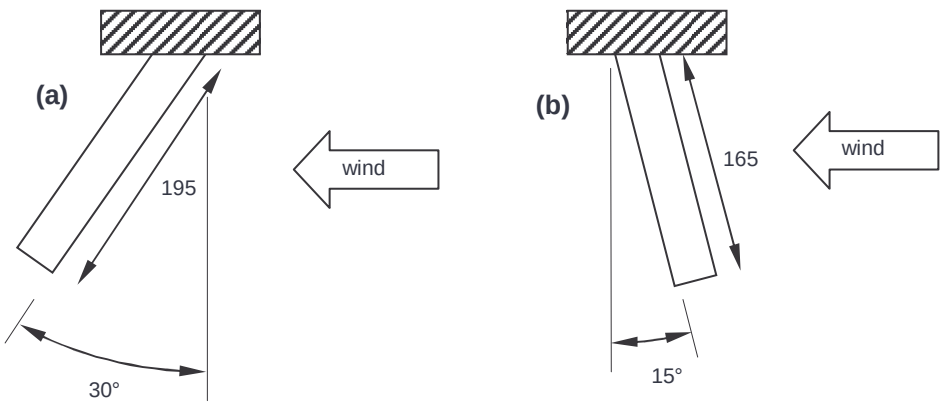

Figure 2. The positions of the wing model: (a) with 30° of sweep angle and (b) with −15° of sweep angle

3. Theoretical model

For comparing its results with the experimental observations a theoretical model, using Kirchhoff plate isoparametric quadrilateral finite elements for the structure and the doublet-lattice method of Albano and Rodden (1969) for the aerodynamics, was constructed. The starting point for the theoretical model construction was the HA145E example given by Rodden and Johnson (1994). The structural grid could represent with relative fidelity the geometry of the ruler in the two positions in which it was placed in the experiments. However, as the side edges of the panels used in the aerodynamic model have to be aligned with the airflow, the ruler tip geometry could not to be faithfully represented in it. Figure 3 shows the grids used for the 30° swept wing. As the geometry represented in the aerodynamic model had to be different of that used in the experiments, there was some freedom to adjust the aerodynamic model geometry in order to improve its results. For the 30° swept wing, the span used (and results are quite sensitive to it) was the one corresponding to the quarter chord line. For the −15° swept wing, the span used in the aerodynamic model was that of the middle chord line. For coupling the aerodynamic and structural models, a single infinite plate spline, of the type described by Harder and Desmarais (1972), was used.

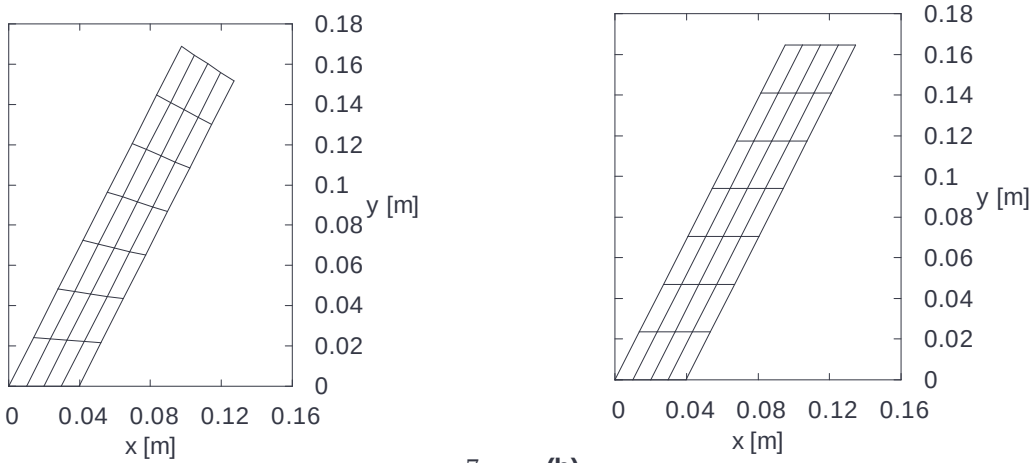

Figure 3. Grids used for the 30° swept wing: (a) structural modeling and (b) aerodynamic modeling

The properties used for modeling the ruler material are listed in Tab. 1. The Young modulus and specific mass are the minimum values given for the sheet grade PVC at the MatWeb (Automation Creations Inc., 2005). The average width of the ruler was around 34.3 mm and the thickness was taken as 0.6 mm, in order to match the measured mass, total length and width of the ruler with the specific mass given for the material. The structural damping was disregarded in the theoretical calculations.

Table 1. Properties used for modeling the ruler material.

Young modulus [GPa]	2.2
Poisson ratio	0.45
specific mass [g/cm^3]	1.3

The first step in the theoretical analysis of aeroelastic instabilities was the normal modes and natural frequencies calculation. This type of calculation was done using the MSC/NASTRAN. The results of this first step were used as input data for the aeroelastic stability analysis, performed using an in-house developed code (Santos *et al*. 2005). The results from the latter code agreed with those furnished by the MSC/NASTRAN aeroelastic analysis module (that was used for verification of the in-house development). This was expected, since the methods implemented are essentially the same in both codes. The results shown in the next section are those of the in-house developed code.

The air specific mass used in calculations (including those used to convert the measured dynamic pressure values in velocities) was that corresponding to the sea level in the International Standard Atmosphere, *i. e.*, 1.225 kg/m^3. The flow was regarded as incompressible, and so the aerodynamic theoretical predictions were made for Mach 0.

4. Results and discussion

Figure 4 shows the ruler, positioned to model the 30° swept wing, before (a) and after (b) it begins to flutter. The change in its behavior is not instantaneous. Intense vibrations at velocities lower than 13.5 m/s were not observed, and

the appearance of the ruler, at these low velocities, was that shown in Fig. 4(a). Between this wind velocity and 14.6 m/s, some vibrations, apparently near the flutter frequency, were observed, but these vibrations seemed to start and stop depending on non-controlled fluctuations of the wind speed. The duration and amplitude or these intermittent vibrations increased with the flow speed, and above 14.6 m/s the vibration was continuous, reaching relatively high amplitudes, as shown in Fig. 4(b), at 15.3 m/s. The photographs shown were taken using an Olympus digital camera C740UZ fixed on a tripod, natural light and 1/6 s of exposure time.

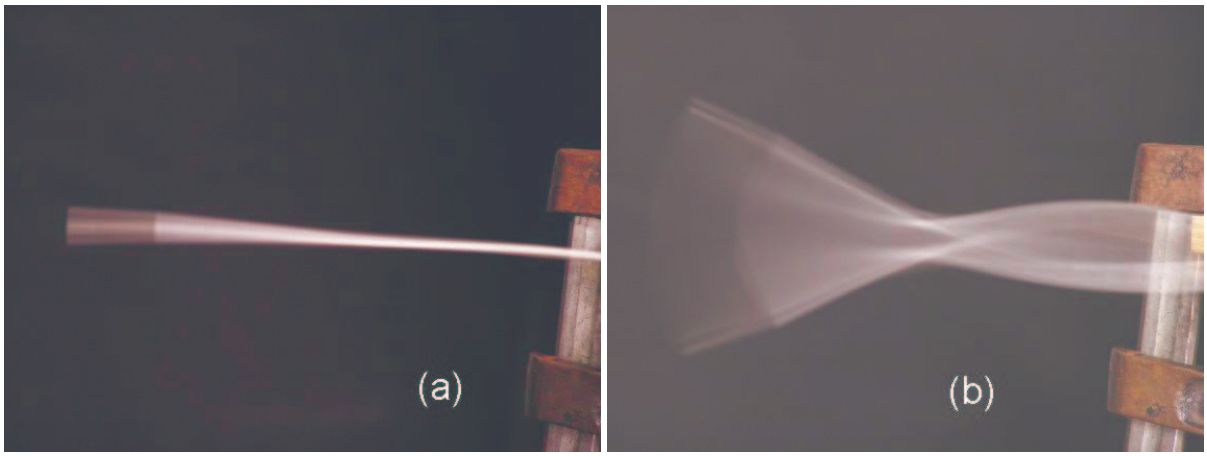

Figure 4. Ruler positioned to represent a 30° sweep angle wing (a) before and (b) after the start of flutter

Figure 5 shows the flutter mode predicted by the theoretical model of the 30° swept wing. It is the result of the coalescence of the first three normal modes of vibration of the structure, in which the second mode is clearly dominant. The first, second and fourth normal modes are basically bending modes, the third is essentially torsion. Comparison of Fig. 5 with Fig. 4(b) shows that the predicted flutter mode is really observed in the experiment.

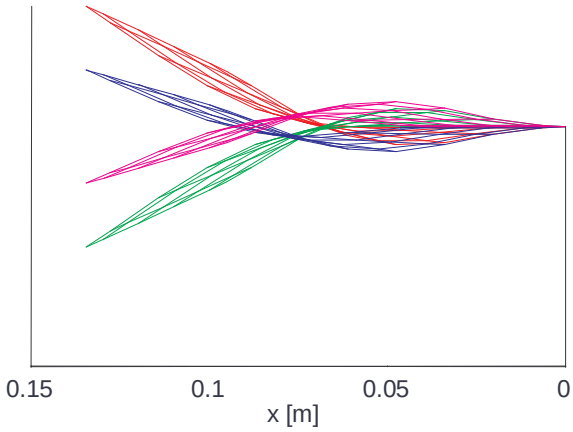

Figure 5. Flutter mode theoretically predicted for the 30° swept wing, shown at four different times

As the calculated flutter modes are vectors of complex numbers (used for representing the phase lag between the different FEM model nodes movement) they can not be represented as a single real function of the spatial coordinates. When the graphs resulting of plotting the flutter mode for some different times are shown together (as done in Fig. 5), however, the resulting picture is not as clear as one could desire. The flutter mode at a single time is shown in Fig. 6, but the perspective may be a source of confusion in this graph – the x and y axes are at the rear side, lines parallel to them, but without tic marks, are in front of them.

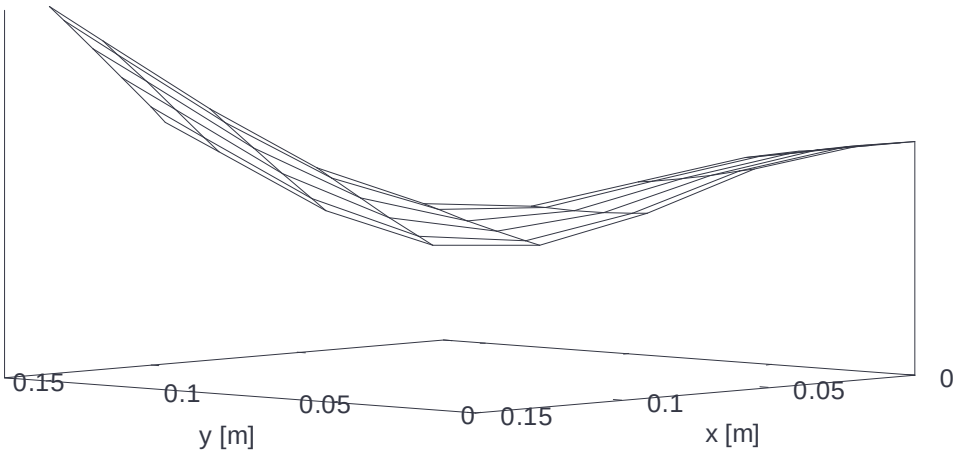

Figure 6. Flutter mode theoretically predicted for the 30° swept wing

Figures 7 and 8 show graphs of frequency (*f*) and coefficient of hysteretic damping (*h*) plotted against the fluid velocity (*V*) as calculated using the KE method[2]. Normally, the *g* letter is used to represent the damping coefficient needed for stabilizing the system, but here, for distinguishing the artificial hysteretic damping calculated by the KE method from the viscous damping calculated by the PK, the *h* letter is adopted, as in Santos *et al.* (2005). The experimental flutter velocity, represented at 14.6 m/s, is not the result of a precise measurement, but a subjective interpretation of the observations described in the first paragraph of this section. The flutter frequency, however, was measured using a digital stroboscope and confirmed using an accelerometer positioned at the ruler support, near the clamping, and a data acquisition/processing system. Both gave the value of 24.3 Hz, and the stroboscope seemed to be the most practical and effective way of measuring the frequency of such high amplitude vibrations of a so light structure (since the accelerometer cannot be fixed directly on the ruler without changing significantly its aerodynamic and weight characteristics, and at the support it does not measure only vibrations due to the ruler movement).

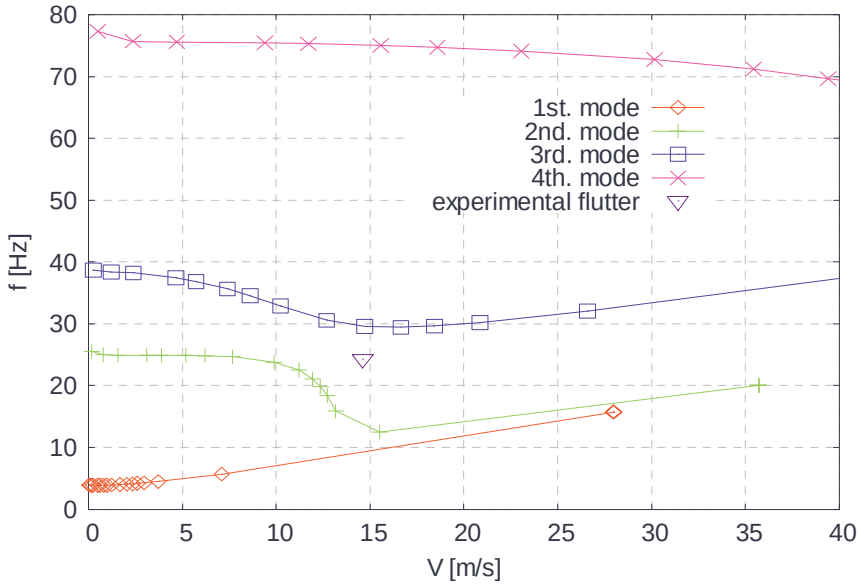

Figure 7. Frequencies *f* corresponding to the 30° swept wing modes of vibration, calculated using the KE method, for different velocities

[2] For obtaining the theoretical aeroelastic stability predictions shown in the present work, the PK and KE methods, in their versions described by Rodden and Johnson (1994), were used.

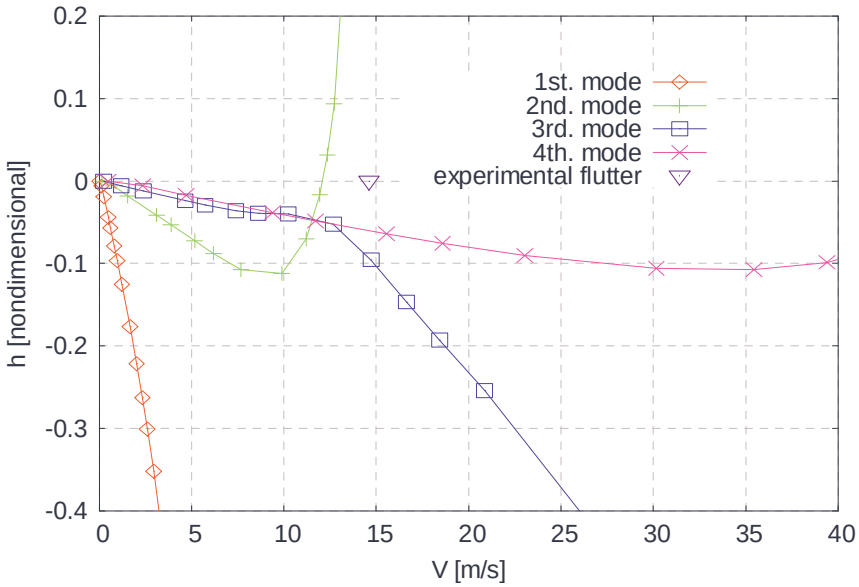

Figure 8. Hysteretic damping coefficients *h* corresponding to the 30° swept wing modes of vibration, calculated using the KE method, for different velocities

Figure 9 shows the ruler, positioned to model the −15° swept wing, before (a) and after (b) the aeroelastic instability manifestation. In this case, the observed instabilities were more difficult to interpret than those of the flutter of the 30° swept wing. For a slightly negative angle of attack, it seemed almost impossible to distinguish, in the experiments, a sign of the static aeroelastic instability, since the aerodynamic loads gradually increase the downward bending of the ruler (that even for null velocity is appreciable, due to the ruler own weight). At this attitude, about 13.5 m/s, a vibration of the ruler (so much deformed that hardly would allow the application of any linear model based on its original geometry) started. For a slightly positive angle of attack, on the other hand, the experimental observations were in better accordance with theory. The photographs shown in Fig. 9 were taken with the wing model at a small positive angle of attack. Figure 9(a) corresponds to a wind velocity around 10.0 m/s, and Fig. 9(b) to a velocity near 11.6 m/s. At some velocity between these two, it was observed a sudden increase in the upward bending caused by the aerodynamic lift. At this velocity range it was difficult to control the wind speed at the facility used, and appreciable velocity fluctuations disturbed the incoming air before it reached the ruler used as wing model. Furthermore, after suffering the high deformation (here interpreted as a form of aeroelastic divergence) the ruler begun to vibrate at a frequency near 33 Hz. The mode of vibration, that can be seen in Fig. 9(b), resembled the torsion represented by the third natural mode predicted theoretically for the ruler clamped with −15° sweep angle in order to represent the wing.

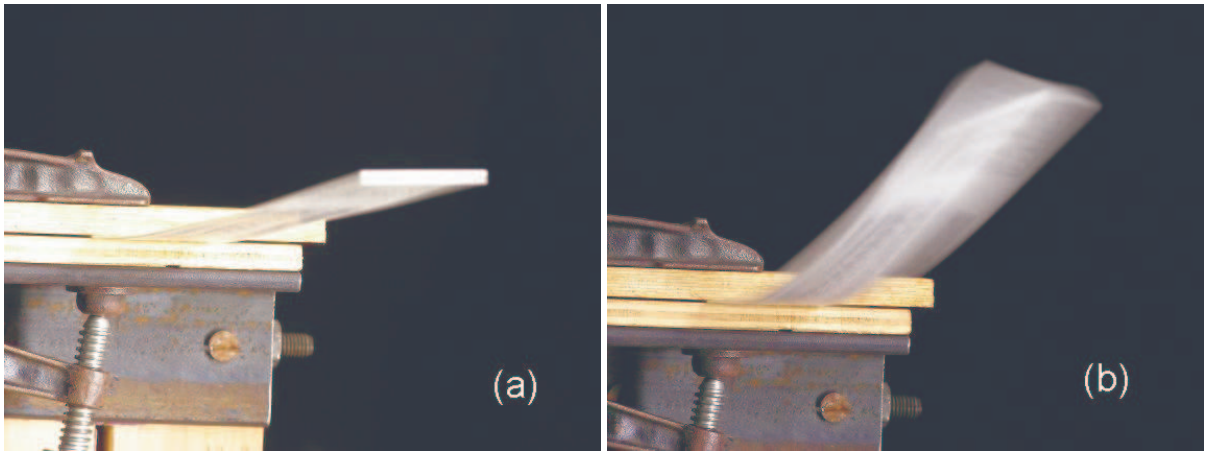

Figure 9. Ruler positioned to model a wing with −15° of sweep angle (a) before and (b) after the aeroelastic instability manifestation

Figures 10 and 11 show graphs of frequency (*f*) and coefficient of damping (*g*) plotted against the fluid velocity (*V*) as calculated using the PK method, regarded as more appropriate for eventually predicting aeroelastic divergence than

the KE method. The experimental aeroelastic instability velocity, represented at 11.6 m/s, was the maximum velocity at which the wing model could remain with small static deformations for a significant time. Above it, the deformations always grew higher, but, as discussed in the preceding paragraph, instabilities were also observed at smaller velocities. The null frequency associated, in Fig. 10, with the instability deserves some explanation as well. Superposed to the high (upward) static deformation, a mode of vibration in torsion at 33 Hz was observed. It must be noted that this 33 Hz value is not far from the predicted third mode flutter frequency (the third mode becomes unstable near 10 m/s, as indicated by the change in sign of the *g*-damping coefficient value needed for stabilizing it, shown in the Fig. 11).

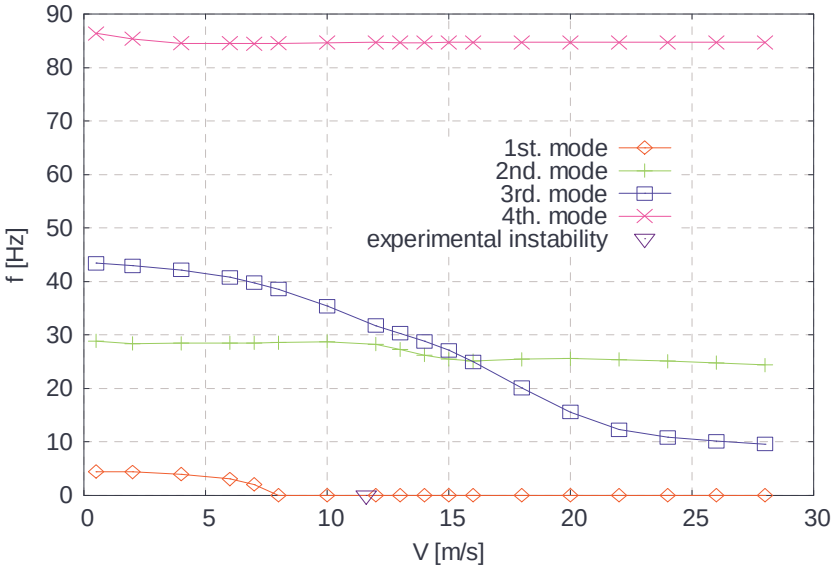

Figure 10. Frequencies *f* corresponding to the −15° swept wing modes of vibration, calculated using the PK method, for different velocities

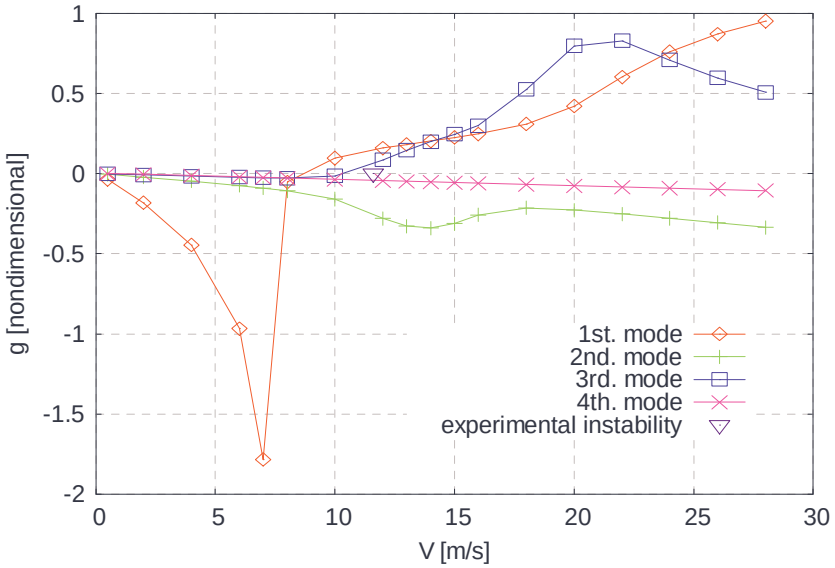

Figure 11. Damping coefficients g corresponding to the −15° swept wing modes of vibration, calculated using the PK method, for different velocities

The linearized theoretical aeroelastic model predicted instability at lower velocities than those in which instability was really observed. This could be expected, since no structural damping was included in the theoretical model and the physical wing model certainly has a structural damping that contributed to retard the appearance of the instabilities. Besides this, nonlinearities played an important role in the experiments here described, specially in those involving the −15° swept wing at negative angle of attack (small deformation assumption breaks down immediately for a structure

that suffers relatively large deformations when subject only to its own weight). Along with geometrical nonlinearities, viscous effects are expected to play an important role in the characteristics of a flow over a wing exhibiting no rounding at its leading edge. Even for a static condition and a small angle of attack, flow separation at the leading edge is likely to occur for such wings. The oscillating motion should reinforce this tendency, increasing the magnitude and alternating the sign of the effective angle of attack on the wing. The situation of a wing, showing pockets of separated flow formed in an alternate way at its upper and its lower surfaces due to its oscillatory motion, could be seen as a *dynamic stall*. A symptom of the stall is the hysteresis observed in the experiments: it was necessary to slow the wind to velocities much lower than those at which the instability started to stop the strong vibration and/or reduce the static deformation associated to the instability.

Finally, it must be noted that it is due to the nonlinearities that the experiments here described could be performed without destroying the ruler used as wing model: the linear theory predicts exponentially growing vibration amplitudes and/or infinite deformations at instability. The limited static deformation and the limit cycle oscillations (LCO) observed were made possible by the nonlinearity of the structural and aerodynamic characteristics of the clamped ruler.

5. Final remarks

The experiments described here could be improved in many ways. Almost all the measurements involved could be made more carefully, their uncertainty could be estimated and the tunnel air stream could be better known and controlled. With a better control over the wind speed, the hysteresis in the instability velocities could be quantitatively evaluated. The clamping of the ruler could also be improved and some vibration tests could be done to measure the dynamic characteristics of the ruler before the wind tunnel tests. And the theoretical analysis could also be refined, specially trying to predict some of the nonlinear effects present in the experiments.

But even without these refinements, the present authors see in the proposed demonstration apparatus a rare opportunity for showing to newcomers on this subject an example of aeroelastic instabilities, the capability of the standard theoretical methods used to predict them, and some of the weaknesses of these methods.

Acknowledgements

The photographs that appear in this paper were kindly produced by the Eng. Fernando Luiz Ferreira de Azevedo. The authors also acknowledge the help of many other colleagues at CTA, specially that of Eng. Matsuo Chiseaki, and are grateful to Eng. Sadahaki Uyeno for lending them his personal photographic tripod.

6. References

Albano, E. and Rodden, W. P., 1969, “A Doublet-Lattice Method for Calculating Lift Distributions on Oscillating Surfaces in Subsonic Flows”, AIAA J., Vol. 7, pp. 279-285.

Automation Creations Inc., 2005, “Overview - PVC, Sheet Grade”, MatWeb Material Property Data, Blacksburg, U.S.A. http://www.matweb.com/search/SpecificMaterialPrint.asp?bassnum=O5609

Collar, A.R.,1978, “The First Fifty Years of Aeroelasticity”, Aerospace, February, pp. 12-20.

Dowell, E.H. (Ed.), Crawley, E.F., Curtiss Jr., H.C., Peters, D.A., Scanlan, R.H. and Sisto, F., 1994, “A Modern Course in Aeroelasticity”, 3rd ed., Ed. Kluwer Academic Publishers, Dordrecht, The Netherlands, 699 p.

Frazer, R. A. and Duncan, W. J., 1931, “ARC R&M 1255 – The Flutter of Monoplanes, Biplanes and Tail Units”, H. M. Stationary Office, London, U.K., 179 p.

Fung, Y.C., 1955, “An Introduction to the Theory of Aeroelasticity”, Ed. John Wiley & Sons, New York, U.S.A., 490 p.

Harder, R.L. and Desmarais, R. N., 1972, “Interpolation Using Surface Splines”, J. Aircraft, Vol. 9, pp. 189-191.

Rodden, W. P. and Johnson, E. H., 1994, “MSC/NASTRAN Aeroelastic Analysis User's Guide (Version 68)”, The MacNeal-Schwendler Corp., Los Angeles, U.S.A.

Santos, L.A., Silva, R.G.A, Castro, B.M., Marto, A.G. and Ponce Alonso, A.C., 2005, “A Planar Doublet-Lattice Code for Teaching and Research in Aeroelasticity”, submitted for publication in the Proceedings of the 18th Brazilian Congress of Mechanical Engineering, Ouro Preto, Brazil.

Templeton, H., 1954, “Massbalancing of Aircraft Control Surfaces”, Ed. Chapman & Hall, London, U.K., 241 p.

Theodorsen, T. and Garrick I.E., 1940, “NACA-TR-685 – Mechanism of Flutter – A Theoretical and Experimental Investigation of the Flutter Problem”, Langley Memorial Aeronautical Laboratory, Langley Field, U.S.A., 46 p.

Theodorsen, T., 1935, “NACA-TR-496 – General Theory of Aerodynamic Instability and the Mechanism of Flutter”, Langley Memorial Aeronautical Laboratory, Langley Field, U.S.A., 21 p.

7. Responsibility notice

The authors are the only responsible for the printed material included in this paper.